THE MODELING OF INITIAL STAGE HYDROGASIFICATION OF VARIOUS RANKED COALS

Edwin J. Hippo
James L. Johnson*

Institute of Gas Technology
3424 S. State
Chicago, Illinois 60616

In the past twenty years, a large effort has been made in the United States to develop commercial coal gasification technology. It has been observed from experimental work that the behavior of coal during the initial stages of coal heat-up, and during a short time interval following heat-up, are crucial to efficiencies of gasification processes. Most carbon oxides, steam, oil and tars, and significant portions of light hydrocarbon gases are evolved during the initial stage. A detailed knowledge of the kinetics of this stage is essential to optimum reactor design.

However, as pointed out previously (1), most studies have been concerned with kinetic correlations of total methane yield after the coal has deactivated to a relatively inert char. On the other hand, this project has been concerned with reactions that take place in the relatively highly reacitve initial stage of transient reactivity, called "rapid-rate methane formation."

Experimental

Details of the reactor system have been presented previously (1). In brief, it is a 1.6 mm diameter, 60 m long helical coiled transport reactor. Nine pairs of electrodes attached along the length of reactor provide an energy source for heating. Temperatures in the nine zones can be adjusted independently to provide constant or linear temperature profiles across the length of the reactor. Coal particles (0.074 to 0.089 mm diameters) are entrained in a gas (hydrogen or helium with less than 0.1% solids by volume) and passed through the reactor. Gas-solid separation occurs in a sintered metal filter (heated to 300°C) at the reactor outlet. Liquids are condensed in a series of cooled traps. The dry gas is analyzed by periodic mass spectrography and by continuous flame ionization. Gases detected have included CO, CO_2, H_2, methane, ethane, and benzene. Proximate and ultimate analyses of coal and chars are determined for each run. Condensible liquids, "heavy hydrocarbons," and steam yields are difficult to determine experimentally because a large surface area is available on which the small yield can condense. Steam yields are determined by oxygen balance, and heavy hydrocarbons are determined by carbon balance.

Isothermal temperatures have varied from 700 to 1040 K, and residence times have been varied up to 13 seconds (depending on the total gas flow rate) for various coals. Maximum temperature for linear temperature profiles range from 700 to 1140 K for constant heating rates of 30, 60, and 80 K/s. A reactor inlet temperature of 590 K was maintained for all constant heating runs. Total operating pressures have ranged from 18 to 52 atmospheres; most runs have been performed at 35 atmospheres.

The gasification kinetics of a Montana lignite, a Montana subbituminous coal, a North Dakota lignite, two Texas lignites, and a Utah subbituminous coal have been investigated. Their proximate and ultimate analyses are included in Table 1. Analyses of coals investigated in other studies (2, 3) are also included. Their gasification behavior will be discussed in terms of the model constructed from the data obtained from the mass transport reactor.

* Deceased.

Table 1. ANALYSES OF THE FEED COALS

Coal	Darco Lignite	Wilcox Lignite	Montana Lignite	North Dakota Lignite	Montana Subbituminous	Illinois No. 6 Bituminous (2)	Utah Subbituminous A	Pittsburg Bituminous (3)	Montana Lignite (3)
Proximate Analysis (Mass %)									
Percentage Ash (Dry)	5.2	25.3	5.15	6.3	8.5	6.0	7.0	11.5	10.6
Percentage Volatile Matter (daf)*	50.8	53.1	45.9	44.9	42.5	39.7	40.9	44.3	44.2
Percentage Fixed Carbon (daf)*	49.2	46.9	54.1	55.1	57.5	60.3	52.1	55.7	55.8
Ultimate Analysis (Dry) (Mass %)									
Percentage Carbon	60.2	47.6	65.13	65.9	67.3	75.45	66.4	68.76	71.2
Percentage Hydrogen	3.49	3.19	4.13	4.19	4.29	5.12	4.14	4.87	5.4
Percentage Nitrogen	0.93	1.14	0.89	0.93	1.07	1.72	1.06	1.32	0.08
Percentage Sulfur (Total)	0.57	1.70	0.57	0.60	1.31	1.32	0.72	5.38	1.32
Percentage Oxygen (By Difference)	29.56	21.01	24.20	22.12	17.58	10.41	20.32	8.21	21.00
	mass %								
O/C (g-atom/g-atom)	0.37	0.33	0.28	0.25	0.20	0.10	0.23	0.09	0.22
H/C (g-atom/g-atom)	0.69	0.80	0.76	0.76	0.74	0.81	0.74	0.85	0.91

* daf = dry ash free.

Typical Results

Typical results for hydrogasification of coals in the mass transport reactor have been reported elsewhere (1). Due to the volume of data collected, only the tentative model for yields of oxygenated species will be discussed in this paper. Models for coal hydrogen evolution have been tentatively proposed and will be presented at a later date.

Previously (4), the evolution of oxygen-containing species during rapid-rate methane formation and devolatilization have been modeled by assuming that a set of reactions occurs to liberate each species. Each set of reactions was represented by a first-order rate equation, but the rate constant had a continuous distribution of activation energies. However, evolved species can arise by different paths. Data scattering and the narrow band of activation energies previously used to fit the data allow a simplifying assumption to be made — namely, that the formation of each species by each route can be represented by a single rate equation containing a single effective activation energy. Thus, the following overall model can be used to fit the data:

$$n_i = \sum_{i,j} \Delta n_{i,j} x_{i,j} \qquad 1)$$

where —

n_i = total amount of species i formed (g-atom of i/g-atom of feed carbon)

$\Delta n_{i,j}$ = maximum amount of species i that can be formed by route j (g-atom of i/g-atom feed carbon)

$x_{i,j}$ = fraction of i converted by route j at any time such that —

$$dx_{i,j}/dt = k_{o_{i,j}} (1 - x_{i,j}) \qquad 2)$$

where —

$k_{o_{i,j}} = k_{o_{i,j}}^{\circ} \exp(-E_{i,j}/RT)$

and —

$k_{o_{i,j}}$ = rate constant for the first order reaction for formation of species i by route j, s^{-1}

$k_{o_{i,j}}^{\circ}$ = pre-exponential factor for the first-order rate equation for the formation of species i by route j

$E_{i,j}$ = activation energy for formation of species i from the coal by route j.

From these assumptions and relationships, the fraction of species i formed can be expressed as —

$$1 - x_{i,j} = \exp\left[- \int_o^{\theta} k_{o_{i,j}}^{\circ} \exp(-E_{i,j}/RT)\, d\theta\right] \qquad 3)$$

for isothermal conversion, and

$$1 - x_{i,j} = \exp\left[-\int_{T_o}^{T_f} \frac{k^{\circ}_{i,j}}{\alpha} \exp\left(-E_{i,j}/RT\right) dT\right] \qquad 4)$$

for a constant heat-up rate condition, where parameters are defined as above and —

T_f = maximum temperature of the coil reactor, K

T_o = entrance temperature of the reactor, K

α = heat-up rate of coal, K/s

Figure 1a reports the carbon dioxide (CO_2) formation and total carbon oxides formation as a function of maximum temperature under constant heat-up and isothermal conditions for Montana and North Dakota lignites gasified in hydrogen. The total carbon oxide yields increase with increasing maximum temperature. CO_2 formation is constant up to 920 K and then decreases with an increase in maximum temperature due to the water-gas shift reaction. The primary CO_2 yield in hydrogen occurs below 755 K, and when corrected for shift, remains constant at higher temperatures. This yield, $n_{CO_2}{}^{H2}$, can be expressed from Equation 1 as —

$$n_{CO_2}{}^{H2} = \Delta n_{CO_2}\, x_{CO_2,0} \qquad 5)$$

where $x_{CO_2,0}$ = 1 for temperatures above 755 K.

The total carbon oxides formed in hydrogen are the sum of the CO and CO_2 formed. Thus, from Equation 1, the total carbon oxides formed in hydrogen can be expressed as —

$$n_{CO + CO_2} = n_{CO_2}{}^{H_2} + n_{CO} \qquad 6)$$

CO formation appears to be derived from one route and the data can be fitted using Equations 3, 4, and 6. The solid lines in Figure 1 represent such a fit for isothermal conditions (line 1) and constant heat-up conditions (line 2).

The total carbon oxides and carbon dioxide yields for the Montana lignite in helium are shown in Figure 1b. Both carbon dioxide and total carbon oxides increase with increasing temperature. In helium, CO_2 formation, $n_{CO_2}{}^{He}$, appears to occur by two paths. One path is described by the model for CO_2 formation in hydrogen; the second path is assumed to be a first-order reaction. Thus, total CO_2 formation can be expressed as:

$$n_{CO_2}{}^{He} = n_{CO_2}{}^{H2} + \Delta n_{CO_2,1}\, x_{CO_2,1} \qquad 7)$$

where $n_{CO_2}{}^{H2}$ has been discussed and $\Delta n_{CO_2,1}\, x_{CO_2,1}$ can be evaluated from the data using Equations 3, 4, and 6. CO formation appears to be the same in helium and in hydrogen. Thus, the total carbon oxide formation in helium can be expressed as:

$$n_{CO + CO_2}{}^{He} = n_{CO_2}{}^{He} + n_{CO} \qquad 8)$$

The solid lines in Figure 1b represent solutions to Equations 3, 4, 7, and 8.

Steam formation can be treated in the same general manner as carbon oxides formation, but data must be corrected for the shift effect. This is done by assuming that primary CO_2 yield in hydrogen is constant above 750 K and that differences between the amount formed by primary gasification and the amount measured are equivalent to the amount of steam formed by the shift reaction. The steam yields for Montana and North Dakota lignites in helium are plotted in Figure 2a, and corrected yields for the two coals in hydrogen are plotted in Figure 2b. A specific amount of steam is formed by one route below 750 K. This "instantaneous" yield can be modeled similar to CO_2 formation below 750 K. This steam yield can be designated $n_{H_2O,o}$. An additional amount of steam is formed in helium by another route above 750 K, such that the total steam yields in helium, $n_{H_2O}^{He}$, are described by —

$$n_{H_2O}^{He} = \Delta n_{H_2O,o}\, x_{H_2O,o} + \Delta n_{H_2O,1}\, x_{H_2O,1} \qquad 9)$$

The lines drawn in Figure 2a were based on the solutions of Equations 3, 4, and 9. Assuming that devolatilization is the same in hydrogen as in helium, it can be seen from Figure 2b that an additional amount of steam formation, beside that predicted by Equation 9, occurs in hydrogen. The amount of oxygen in the additional steam is equal to the amount of oxygen in the increased CO_2 yield in helium. Thus, in hydrogen, a certain fraction of coal-oxygen is evolved as steam by an assumed first-order reaction that inhibits CO_2 formation, which would otherwise occur in an inert atmosphere. Again the additional steam yield is modeled by a first-order rate equation, and the total steam yield in hydrogen can be modeled by —

$$n_{H_2O}^{H_2} = n_{H_2O}^{He} + \Delta n_{H_2O,2}\, x_{H_2O,2} \qquad 10)$$

The solid lines in Figures 2a and 2b are solutions to Equations 3, 4, 9, and 10 for the different coals considered.

The total oxygen evolved from coal can be estimated as the sum of oxygen evolved as CO, CO_2, and H_2O. Curves for predicted coal-oxygen evolution for the Montana and North Dakota lignites in hydrogen under isothermal and constant heat-up conditions are included in Figure 3a. Actual data are also reported to show the close fit. A similar plot of oxygen yield as a function of temperature, shown in Figure 3b, reveals that the model developed for oxygen evolution in helium fits the data for helium gasification of a Montana lignite.

Table 2 lists the kinetic parameters that were used to generate the solid lines in Figures 1 through 3. Note that the parameters are not listed for the "instantaneous" formation of CO_2 and steam (below 750 K) because rate data were not obtained at these temperatures.

Table 2. KINETIC PARAMETERS FOR EVOLUTION OF OXYGENATED SPECIES FROM COALS

Volatile Component	Pre-Exponential Factor k_o°, s^{-1}	Activation Energy E (kcal/mol)
$n_{CO_2,1}$	2.0×10^5	27.83
$n_{H_2O,1}$	5.42×10^9	38.89
$n_{H_2O,2}$	6.45×10^9	44.98
n_{CO}	5.47×10^5	25.80

The evolution of CO, CO_2, and H_2O can be correlated with coal rank. The plots of maximum volatile yields in hydrogen of CO, CO_2, and H_2O, expressed as g-atom oxygen yield per g-atom feed carbon, versus coal rank (expressed as g-atom oxygen per g-atom carbon in the raw coal), are approximately straight lines (Figure 4). These yields are closely related to various functional groups in the coal. For example, CO_2 corrected for shift can be shown to have the following relationship:

$$\Delta n_{CO_2} = n_{carboxyl}(5) = 0 \text{ for } n_o^\circ < 0.1 \qquad 11)$$

$$\Delta n_{CO_2} = 0.4\ (n_o^\circ - 0.1) \text{ for } n_o^\circ \geq 0.1 \qquad 12)$$

where —

Δn_{CO_2} = maximum CO_2 yield (g-atom oxygen/g-atom of feed carbon)

n_o° = total oxygen in raw coal (g-atom O/g-atom carbon)

$n_{carboxyl}$ = total carboxyl oxygen in raw coal (g-atom O/g-atom coal C).

Steam yields can be expressed as —

$$\Delta n_{H_2O} = n_{hydroxyl}(5) = 0.65\ (n_o^\circ) \text{ for } n_o^\circ \leq 0.23 \qquad 13)$$

$$\Delta n_{H_2O} = 0.13 + 2\ (n_o^\circ - .23) \text{ for } n_o^\circ \geq 0.23 \qquad 14)$$

where —

Δn_{H_2O} = maximum steam yield (g-atom O/g-atom feed carbon)

$n_{hydroxyl}$ = hydroxyl oxygen in raw coal (g-atom O/g-atom coal carbon).

Carbonyl oxygen forms CO exclusively, as can be seen in the following correlations:

$$n_{carbonyl}(5) = 0.32\ (n_o^\circ - 0.1)\ n_o^\circ > 0.1 \qquad 15)$$

$$\Delta n_{CO} = 0.31\ (n_o^\circ - 0.1)\ n_o^\circ > 0.1 \qquad 16)$$

where —

Δn_{CO} = maximum CO yield (g-atom O/g-atom feed carbon)

$n_{carbonyl}$ = carbonyl oxygen in feed coal (g-atom O/g-atom feed carbon).

Thus, it appears that volatile yields containing oxygen can be estimated from a single parameter: coal rank expressed as the O/C ratio.

Using the above model and the maximum yields of individual products measured for each coal, yields at the various maximum temperatures can be predicted with the aid of Equations 1-10. These models also predict behavior for hydrogasification of a Illinois No. 6 bituminous coal (2) and pyrolysis of a lignite and Pittsburgh No. 9 bituminous coal (3).

Figure 5 presents a comparison of the predicted total oxygen yields from Equation 1-10 and the actual experimental yields for the various coals gasified under a variety of conditions. Similar plots for carbon oxides in hydrogen, carbon oxides in helium, steam in hydrogen, and steam in helium, can be made. The correlations are adequate in predicting yields of oxygenated species for given temperature histories in most cases.

In summary, even though the hydrogasification is not completely understood, it can be seen that significant strides have been made in identifying individual reaction paths that contribute to the gasification phenomena.

References Cited

1. Johnson, J. L., "Kinetics of Initial Coal Hydrogasification Stages," ACS Fuel Abstracts 22, No. 1, 17-37 (1977) March.

2. Feldmann, H. F., Mina, J. A. and Yavorsky, P. M., "Pressurized Hydrogasification of Raw Coal in a Dilute-Phase Reactor," Adv. Chem. Ser. 131 (1974).

3. Suuberg, E. M., "Rapid Pyrolysis and Hydropyrolysis of Coal," Ph.D. Thesis, Massachusetts Institute of Technology, August 1977.

4. Johnson, J. L., "Kinetics of Devolatilization and Rapid Rate Methane Formation," 1975 Annual Report to A.G.A. from Institute of Gas Technology, Project IU-4-11.

5. Van Krevelen, D. W., Coal Science, Elsevier, Amsterdam, 1961.

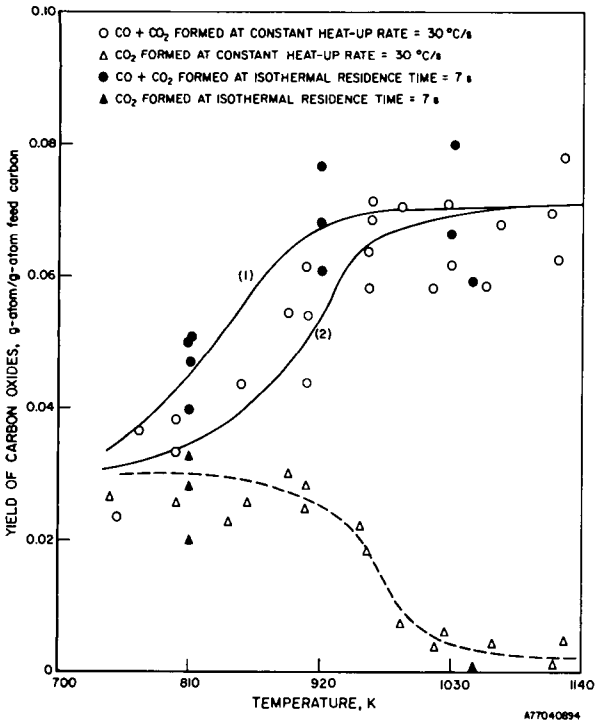

Figure 1a. Yields of Carbon Oxides for Montana and North Dakota Lignites in Hydrogen

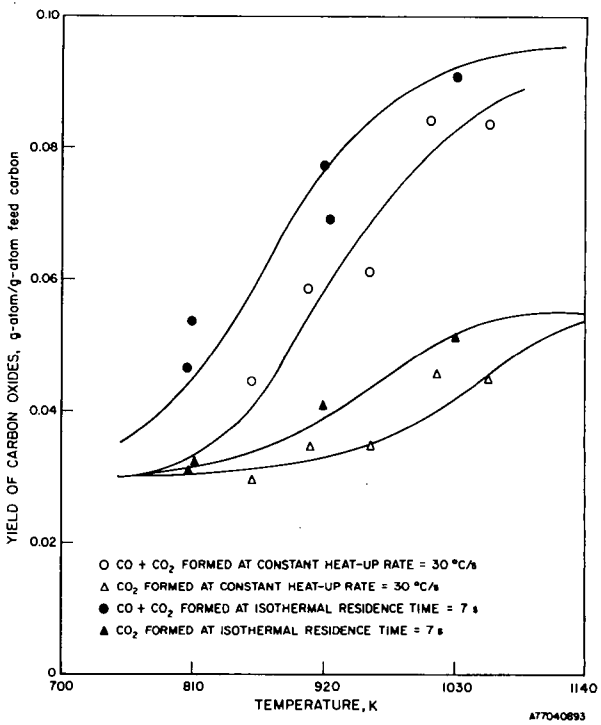

Figure 1b. Carbon Oxides Yields for Montana Lignite in Helium

Figure 1. PREDICTED AND ACTUAL CARBON OXIDE YIELDS FOR MONTANA AND NORTH DAKOTA LIGNITES

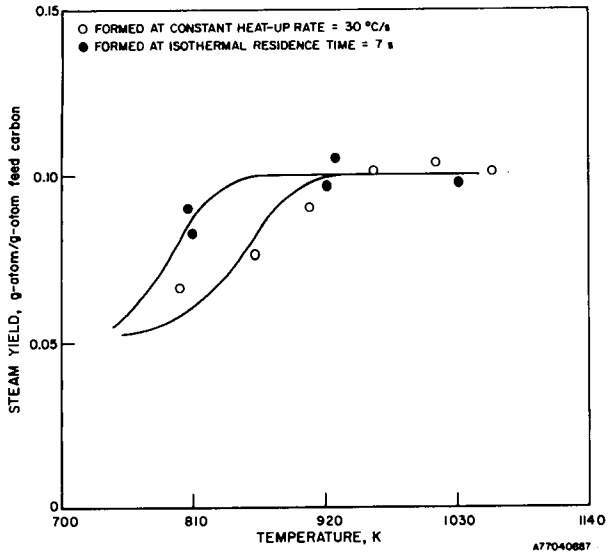

Figure 2a. Steam Yields for Montana and North Dakota Lignites in Hydrogen

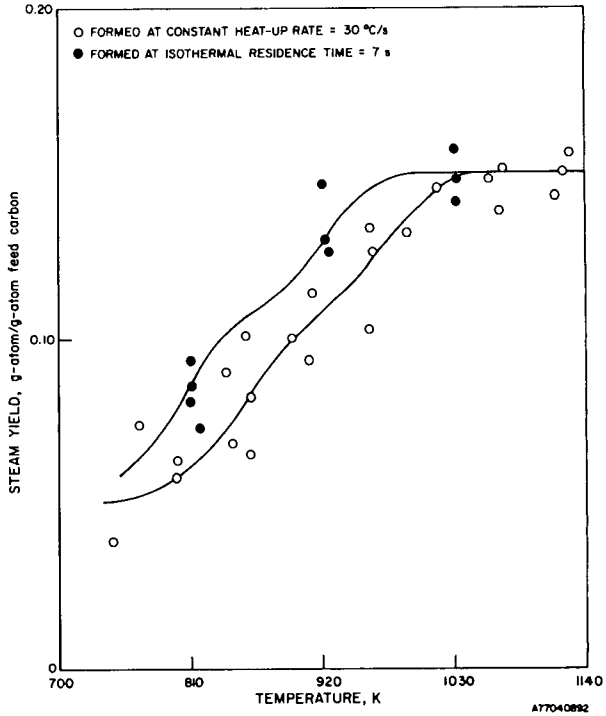

Figure 2b. Steam Yields for Montana Lignite in Helium

Figure 2. PREDICTED AND ACTUAL STEAM YIELDS FROM MONTANA AND NORTH DAKOTA LIGNITES

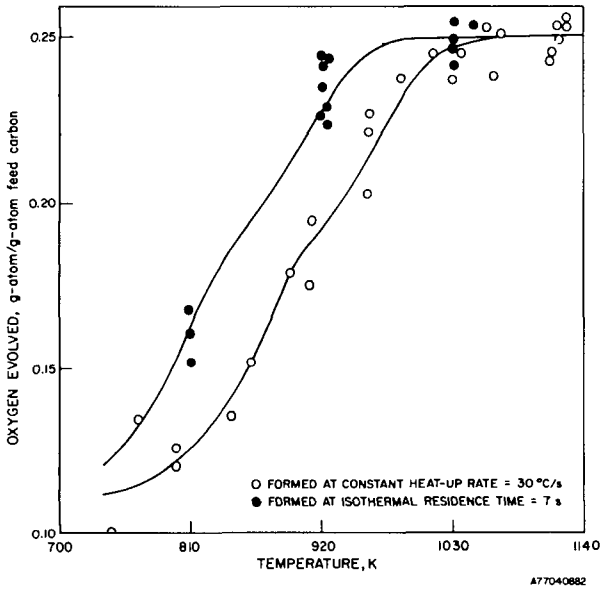

Figure 3a. Total Oxygen Evolved From a Montana and a North Dakota Lignite in Hydrogen

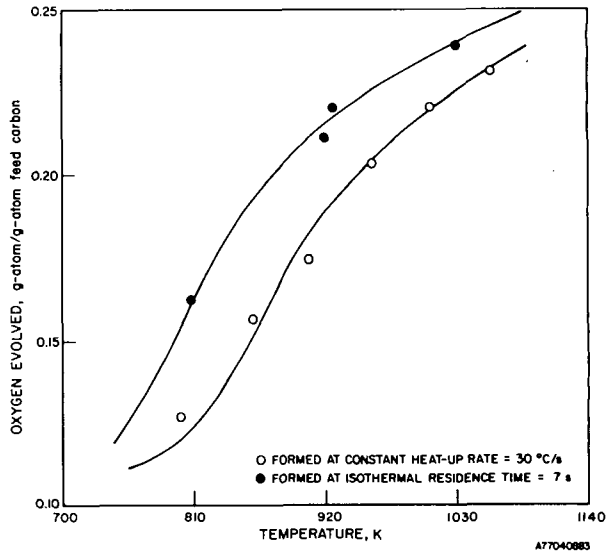

Figure 3b. Oxygen Evolved From Montana Lignite in Helium

Figure 3. PREDICTED AND ACTUAL COAL OXYGEN GASIFIED FROM MONTANA AND NORTH DAKOTA LIGNITE

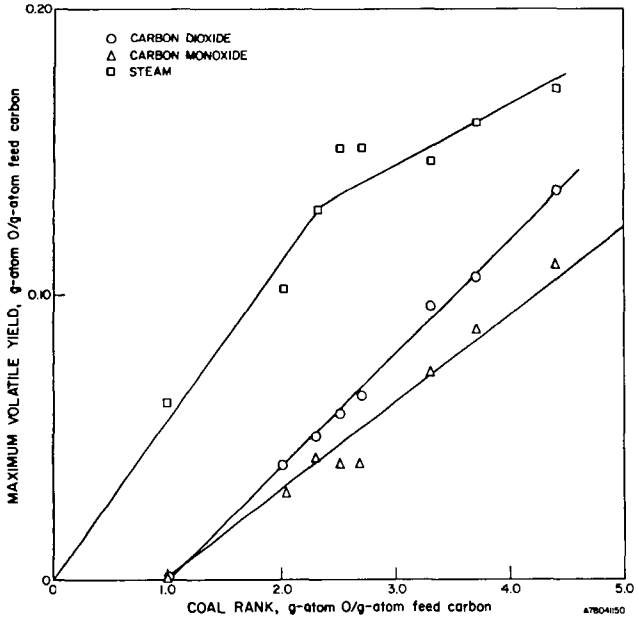

Figure 4. CORRELATION BETWEEN COAL RANK AND VOLATILE YIELDS

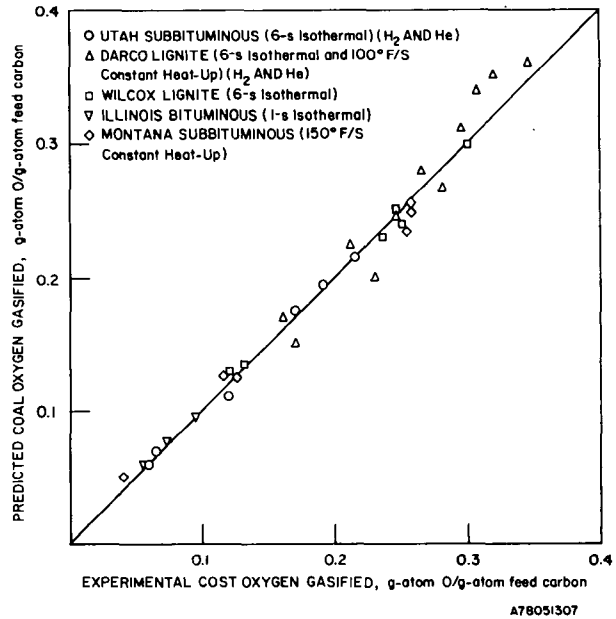

Figure 5. COMPARISON OF PREDICTED AND EXPERIMENTAL YIELDS OF TOTAL COAL OXYGEN GASIFIED FROM VARIOUS COALS UNDER A RANGE OF CONDITIONS